MZM nonlinear equalization by sinusoidal subcarrier modulation combined with LM-BP neural network*

LI Li and WANG Zijun**

College of Communication Engineering, Jilin University, Changchun 130012, China

(Received 15 November 2023; Revised 3 April 2024)

In order to mitigate the nonlinear effects of Mach-Zehnder modulator (MZM) on optical transmission signals in intensity modulation and direct detection (IM-DD) systems, a combined approach utilizing sinusoidal subcarrier modulation (SSM) and the Levenberg-Marquardt back propagation (LM-BP) neural network is proposed in this paper. The method employs a sine wave as the subcarrier to carry the 4 pulse amplitude modulation (PAM4) signals, aiming to equalize the distorted signals after MZM modulation. Subsequently, the LM-BP algorithm eliminates any remaining inter-symbol interference (ISI). This scheme uses sine wave modulation to solve the problem of additional ISI caused by triangular wave modulation. Furthermore, this combined approach simplifies the algorithm complexity compared to solely relying on a neural network equalizer. In this paper, the performance of SSM-LM-BP scheme is simulated and analyzed in IM-DD system. The results show that the joint scheme outperforms the triangular wave modulation scheme as well as the neural network algorithm after transmitting 50 Gbit/s PAM4 signals for 80 km without relays under the conditions of dispersion compensation, and the symbol error rate (*SER*) can be as low as 10^{-5}.

Document code: A **Article ID:** 1673-1905(2024)10-0592-7

DOI https://doi.org/10.1007/s11801-024-3252-9

For considerations of flexibility and cost in large-scale deployment, optical communications based on intensity modulation and direct detection (IM-DD) system have been widely studied for data center interconnection in short-distance optical links. However, facing the application scenario of increasing data traffic, the modulation format non-return-to-zero (NRZ) of the traditional IM-DD system is difficult to meet the requirements of transmission capacity upgrading, and the next-generation IM-DD system integrates higher-order modulation formats with digital signal processing technology to achieve the high-speed transmission[1-4]. In IM-DD systems, the Mach-Zehnder modulator (MZM) has become a widely used electro-optical modulator due to its broad modulation bandwidth and fast modulation rate. Nevertheless, the inherent modulation characteristics of the MZM introduce signal nonlinear distortion, which is an inevitable issue. Therefore, this paper conducts a systematic investigation into the primary factors contributing to MZM nonlinearity and proposes compensation methods.

In order to compensate the nonlinearity of MZM, NAVID et al[5] proposed an electron pre-distortion-based broadband linearization method that utilizes second-order intermodulation (IM2) products injected into distributed amplifiers to compensate for MZM nonlinearities and to improve the spurious-free dynamic range (SFDR). But it is complicated to realize. Ref.[6] used a signaling scheme with a triangular wave as a subcarrier for suppressing the nonlinear interference generated by MZM on the signal during the modulation process. However, because of the existence of fundamental and odd harmonic components in the triangular wave, its inclusion makes the system equalize the nonlinearities while bringing additional inter-code crosstalk, and requires more accurate amplitude regulation. LUO et al[7] designed the first CMOS MZM driver capable of operating over a wide frequency range of 20—35 GHz using a programmable linearization circuit. The linearization circuit, consisting of an inverter-based amplifier segment, is utilized to provide programmable pre-distortion gain over the input signal region to suppress the nonlinear distortion of the MZM. The modulation process is computationally complex and costly and is not applicable to practical IM-DD systems. Furthermore, digital signal processing techniques are often employed as the central solution to compensate for the nonlinear distortions that occur in signals when they are transmitted through modulators. Volterra nonlinear equalizer (VNLE) is one of the most popular nonlinear equalizer techniques in the field of digital signal processing (DSP), as it can model complex nonlinear functions. Although VNLE effectively mitigates most nonlinear distortions, it often

* This work has been supported by the National Key Research and Development Program of China (No.2020YFB1805805).

** LI Li is an associate professor at the College of Communication Engineering, Jilin University. She received her Ph.D. degree in 2009 from Jilin University. Her research interests are mainly in communications signal processing. E-mail: LL@jlu.edu.cn

entails high computational complexity[8-10]. In recent years, neural network algorithms have also been widely utilized to equalize such nonlinearities[11,12]. But the complexity of neural network equalizers is also not low, and it can be challenging to achieve superior compensation for larger nonlinearities.

Therefore, the nonlinear impairments caused by MZM remain a significant challenge that needs to be addressed. In this paper, we present an MZM nonlinear equalization scheme based on sinusoidal subcarrier modulation and the Levenberg-Marquardt back propagation (SSM-LM-BP) for IM-DD system, aiming to mitigate the nonlinear interference of MZM. The sinusoidal subcarrier is used because the transfer function of the MZM is cosine-like and the frequency component of the sinusoidal waveform is relatively single, which will not cause the system to generate additional inter-symbol interference (ISI). In this paper, we analyze the source of the nonlinear impairments of the MZM, the electro-optical modulation process of the sinusoidal subcarrier in the MZM, and the equalization principle of the neural network algorithm and carry out the theoretical derivation, and we compare the equalization effects of the LM-BP algorithm, SSM and the joint scheme. The simulation results show that the LM-BP algorithm can only compensate for small nonlinearities, while the SSM scheme can significantly reduce the nonlinear effects of MZM on the signal. Consequently, the combined scheme achieves effective nonlinear compensation for the system while significantly reducing the computational complexity associated with neural network algorithm.

In ideal conditions, the optical signal input to the MZM is evenly split into two paths by the Y-branch, with each path carrying half the power. These two paths of light propagate through the optical waveguides of the upper and lower arms of the MZM, and the phase of the light passing through them is changed by varying the voltage across the optical waveguides of the two arms. Subsequently, another Y-branch the output recombines the phase-modulated light waves into the output of the MZM.

Here assume that the light field intensity of the optical signal input to the MZM is $E_{\text{in}}(t)$, the output light field intensity of the MZM is $E_{\text{out}}(t)$, and the driving voltages on the two arms of the MZM are $v_1(t)$ and $v_2(t)$, and the relationship between the MZM input light field intensity and the output light field intensity can be expressed as

$$E_{\text{out}}(t)=\frac{E_{\text{in}}(t)}{10^{IL/20}}\left[\gamma \mathrm{e}^{\mathrm{j}\varphi_1}+(1+\gamma)\mathrm{e}^{\mathrm{j}\varphi_2}\right], \tag{1}$$

where IL is the parameter insertion loss, γ denotes the power splitting ratio of the two Y-branch waveguides, $\gamma=\left(1-1/\sqrt{10^{ExtRatio/10}}\right)/2$, where $ExtRatio$ is the extinction ratio. φ_1 and φ_2 are the optical phases of the upper and lower arms of the MZM, which are controlled by the driving voltages loaded on the two arms, given by Eqs.(2) and (3), respectively. v_{bias1} and v_{bias2} are the bias voltages of the upper and lower arms, respectively, $v_{\pi\text{RF}}$ is the switching modulation voltage, and $v_{\pi\text{DC}}$ is the switching bias voltage.

$$\varphi_1=\frac{\pi v_1(t)}{v_{\pi\text{RF}}}+\frac{\pi v_{\text{bias1}}}{v_{\pi\text{DC}}}, \tag{2}$$

$$\varphi_2=\frac{\pi v_2(t)}{v_{\pi\text{RF}}}+\frac{\pi v_{\text{bias2}}}{v_{\pi\text{DC}}}. \tag{3}$$

Then the relationship between the input electric field intensity and the output electric field intensity of the MZM can be expressed as

$$E_{\text{out}}(t)=\frac{E_{\text{in}}(t)}{10^{IL/20}}[\gamma\exp(\mathrm{j}\pi v_1(t)/V_{\pi\text{RF}}+\mathrm{j}\pi v_{\text{bias1}}/V_{\pi\text{DC}})+(1-\gamma)\exp(\mathrm{j}\pi v_2(t)/V_{\pi\text{RF}}+\mathrm{j}\pi v_{\text{bias2}}/V_{\pi\text{DC}})]. \tag{4}$$

In IM-DD systems utilizing 4 pulse amplitude modulation (PAM4) signals, nonlinear impairments resulting from variations in the bias voltage can lead to distortion in the eye diagram of the PAM4 signal. For this study, the Optisystem simulation software was utilized for conducting simulation experiments. The MZM had an extinction ratio of 20 dB, a switching bias voltage of 4 V, a switching modulation voltage of 4 V, and an insertion loss of 5 dB. Fig.1 shows the eye diagrams of the simulated distortion of the MZM by changing the bias voltage.

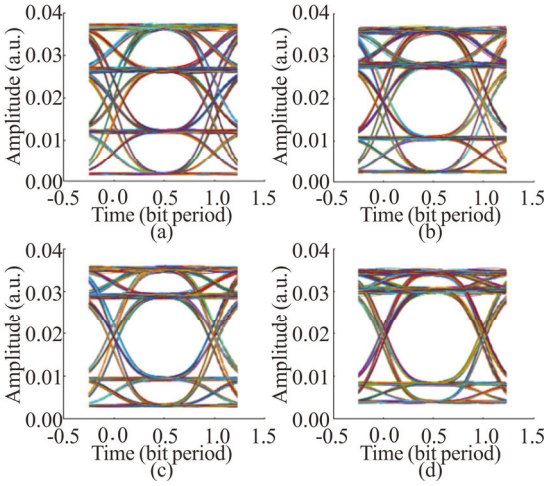

Fig.1 Eye diagrams of simulated MZM distortion by varying bias voltage: (a) V_{bias1}=3 V, V_{bias2}=−1.4 V; (b) V_{bias1}=3 V, V_{bias2}=−1.3 V; (c) V_{bias1}=3 V, V_{bias2}=−1.2 V; (d) V_{bias1}=3 V, V_{bias2}=−1.1 V

It can be seen that the eye in the middle of the eye diagram gradually increases with increasing v_{bias2}, as a way of modeling the gradual increase in nonlinear distortion of the MZM.

The relationship between the MZM input light field intensity and the output light field intensity can likewise be as

$$E_{\text{out}}(t)=\frac{E_{\text{in}}(t)}{1+\gamma}\{\gamma\exp[-(-\Delta\alpha_\alpha(v_1(t)/2)+$$

$$j\Delta\beta v_1(t))L]+\exp[-(\Delta\alpha_\alpha(v_2(t)/2)+j\Delta\beta v_2(t))L]\}, \quad (5)$$

where $\Delta\alpha_\alpha/2$ is the attenuation constant, $\Delta\beta$ is the phase constant, and L is the interaction length of the modulator arms.

The nonlinear distortion of the MZM can also be simulated by varying the absorption and phase of the optical signal in each arm of the MZM in relation to the applied voltage. To obtain the absorption and phase of the optical signal in each arm of the MZM in relation to the applied voltage, either a direct measurement of the straight cross section of the waveguide cut from one of the arms of the modulator can be conducted, or the cosine rule can be utilized along with measurements of the output signal intensity of each arm in relation to the voltage. This voltage relationship is obtained. In this study, the Optisystem simulation software is utilized once again for simulation experiments. The splitting ratio is set to 1: 1, with v_{bias1} of −2.2 V and v_{bias2} of −1.4 V.

A file of the nonlinear functions of the absorption and phase of the optical signals of each arm of the altered MZM with respect to the applied voltage is written to the MZM module, and Fig.2 shows the nonlinear plots of the absorption and phase of the optical signals of each arm of the altered MZM as a function of the applied voltage for four groups. Fig.3 shows the corresponding eye diagrams for the four groups.

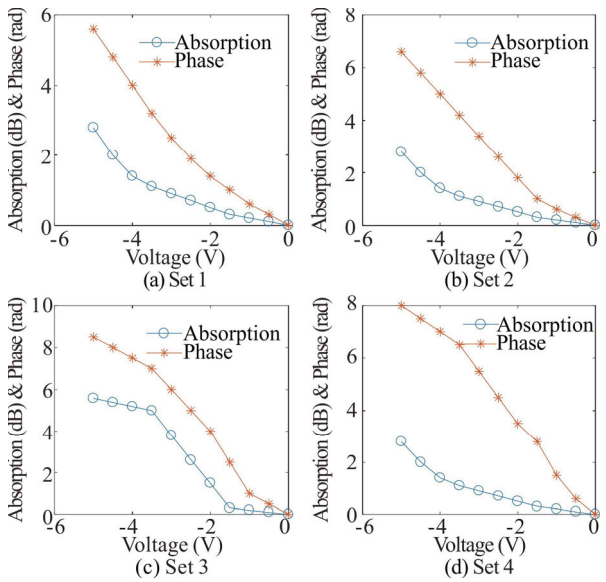

Fig.2 Four sets of nonlinear plots of the absorption and phase of the optical signal in each arm of the altered MZM as a function of the applied voltage

The eye diagrams of the two simulated nonlinearities show that both the change in bias voltage and the change in absorption and phase of the optical signal in each arm of the modulator with the applied voltage are ultimately changes in the amplitude and phase of the signal, which ultimately turn into aberrations in the level of the eye diagram.

The structure of the MZM nonlinear compensation based on SSM is depicted in Fig.4. Initially, a pseudo-random bit sequence generator is employed to generate a segment of random binary digital signal. Subsequently, a PAM sequence generator is utilized to map this random signal into the PAM4 signal format. At this stage, each symbol of the signal carries 2 bits of information.

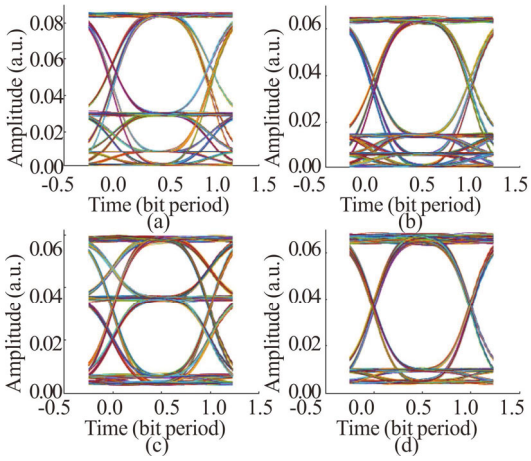

Fig.3 Four sets of eye diagrams corresponding to Fig.2

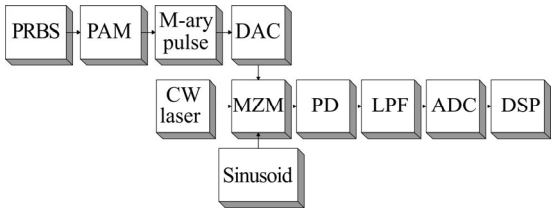

Fig.4 Structure of MZM nonlinear compensation based on sinusoidal subcarrier modulation

The PAM4 signal, after mapping, enters the multilevel pulse generator for pulse shaping, generating a digital signal. This digital signal then passes through a digital-to-analog converter (DAC) where it is converted to an analog signal. The PAM4 signal, after digital-to-analog converted, along with the sine wave, simultaneously enters the MZM. Both signals are then driven by the laser for photoelectric conversion.

The continuous laser generates a continuous optical signal $E_{in}(t)=E_0\exp(j\omega_0 t+\varphi_0)$ with an amplitude of E_0, an angular frequency of ω_0, and an initial phase of φ_0, and the subcarrier is a sinusoidal signal $s(t)=A\sin(\omega t+\varphi)$ with an amplitude of A, an angular frequency of ω_1, a time of t, and an initial phase of φ. That is, after the MZM modulation, the output optical signal can be expressed as

$$E_{out}(t)=\frac{E_{in}(t)}{10^{IL/20}}\left[\gamma s(t)e^{j\varphi_1}+(1+\gamma)e^{j\varphi_2}\right]=$$

$$\frac{E_{in}(t)}{10^{IL/20}}\left[\frac{A}{2}\gamma e^{j(\varphi_1+\Delta\varphi)}+(1+\gamma)e^{j\varphi_2}\right], \quad (6)$$

$$\Delta\varphi = \frac{\pi}{2} - (\omega t + \varphi). \tag{7}$$

The conversion of a sine wave signal into a cosine wave only requires a change of π/2 phase. According to Eqs.(6) and (7), it can be seen that the added sine wave is to change the phase of one arm of the MZM, so it is only necessary to change the amplitude and phase of the added sine wave accordingly to compensate for the distorted signal due to the nonlinearity of the MZM.

After adding the subcarrier photoelectric conversion of the optical signal is converted into an electrical signal by a photodetector (PD). The current generated by the PD varies with the incident optical power, and the output current of the PD at the receiving end is positively correlated with the square of the received optical field intensity and can be expressed as

$$I_{\text{out}} \propto \left|E_{\text{out}}(t)\right|^2. \tag{8}$$

The converted electrical signal containing the subcarrier signal is filtered by a low-pass Gaussian filter to filter out the high-frequency component to obtain the nonlinearly compensated PAM4 signal, and the filter transfer function can be expressed as

$$H(f) = \alpha \exp\left[-\ln\left(\sqrt{2}\right)\left(\frac{f}{f_c}\right)^{2N}\right], \tag{9}$$

where α is the insertion loss, f_c is the filter cutoff frequency, f is the frequency, and N is the filter order.

Next, the nonlinearly compensated PAM4 signal is converted into a digital signal by an analog-to-digital converter (ADC). Finally, the compensated signal is subjected to digital signal processing using a neural network algorithm to equalize the ISI.

The artificial neural network (ANN) can easily approximate nonlinear functions and exhibits strong nonlinear representation capabilities. Artificial neural network based on nonlinear equalizer (ANN-NLE) has been demonstrated to effectively handle both linear and nonlinear impairments in various types of directly detected short-range intensity modulation systems[13].

The BP algorithm is a supervised learning algorithm commonly used to train multilayer perceptron machines. The middle layer of the neural network structure serves as the hidden layer, whose primary function is to represent the relationship between inputs and outputs using a weighted linear summation function. In PAM4-based fiber optic communication system, as the nonlinear impairments that require compensation are limited, it suffices to have only one hidden layer in the neural network and an output node in the output layer to perform the summation of the output values. This BP neural network model is designed to meet the performance requirements of typical optical transmission system with limited complexity.

The nonlinear fitting capability of the BP neural network equalizer heavily relies on the structure of the equalizer neural network. In optical communication system, signal nonlinearities are typically limited, thus the hidden layer of the neural network is often set to a single layer. In this configuration, the neural network assumes a three-layer structure consisting of an input layer, hidden layer and output layer, as shown in Fig.5.

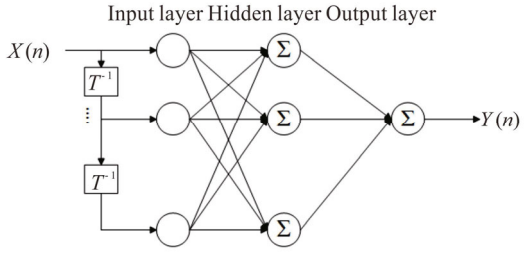

Fig.5 BP neural network model

The output signal $y(n)$ can be calculated as

$$y(n) = f\left(b + \sum_{i=1}^{r} w_i \sigma\left(b_i + \sum_{j=0}^{m-1} w_{ij} x(n-j)\right)\right), \tag{10}$$

where the vector $x(n)$ denotes the input signal, the neural network weights w_{ij} and w_i denote the connection weights from the jth node in the input layer to the ith node in the hidden layer, and the weights between the ith node in the hidden layer to the output layer, respectively; the deviations b_i and b denote the deviations of the ith node in the hidden layer and the output node in the output layer, respectively; the integers m and r denote the numbers of nodes in the input layer and the hidden layer, respectively.

The sigmoid function is used for the activation function of the hidden layer and can be expressed as

$$f(x) = \frac{1}{\left(1 + \mathrm{e}^{-x}\right)}. \tag{11}$$

The process of neural network training data involves continuously adjusting the unknown parameters to minimize the cost function. Common computational algorithms for this purpose include the gradient method, Newton's method, and the LM method. In order to update the weights of the neural network connections, the LM algorithm is used here. The LM algorithm aims to find the weights of connected neurons when the derivatives are zero, and its structure is similar to Newton's method, making it significantly faster than the traditional gradient descent algorithm. In addition, the LM algorithm actually belongs to a class of algorithms for least squares computation with a nonlinear cost function[14].

Set the allowable value of training error ε, the constants μ and β ($0<\beta<1$) and initialize the weights and threshold vector, so that the number of iterations k=0. The error function of the network correcting the weights can be expressed as

$$E(w^k) = \frac{1}{2}\sum_{i=1}^{P}\left\|Y_i - Y_i'\right\| = \frac{1}{2}\sum_{i=1}^{P} e_i^2(w^k), \tag{12}$$

where Y_i is the desired network output vector, Y_i' is the actual network output vector, P is the number of samples,

w is the vector consisting of network weights and thresholds, and $e_i(w^k)$ is the error between the desired network output and the network output of the kth iteration. w^k denotes the vector consisting of the weights and thresholds of the kth iteration, the vector consisting of the new weights and thresholds $w^{k+1}=w^k+\Delta w$, and the weight increment w is calculated as

$$\Delta w=\left[\boldsymbol{J}^{\mathrm{T}}(w)\boldsymbol{J}(w)+\mu\boldsymbol{I}\right]^{-1}\boldsymbol{J}^{\mathrm{T}}(w)e(w), \tag{13}$$

where $\boldsymbol{I}$ is the unit matrix, μ is the user-defined learning rate, and $\boldsymbol{J}(w)$ is the Jacobian matrix.

According to the relationship between the error value and the error allowable value, determine whether the learning is over. If $E\left(w^k\right)<\varepsilon$, the training and learning is over; if $E\left(w^k\right)\geq\varepsilon$, the error function is computed with $w^{k+1}=w^k+\Delta w$ as the weights and threshold vectors; if $E\left(w^{k+1}\right)<E\left(w^k\right)$, make $k=k+1$, $\mu=\mu\beta$, and repeat the computation of the error function of the network to correct the weights $E\left(w^k\right)$; otherwise $\mu=\mu/\beta$, and repeat the computation of the weights increment Δw.

During the training process, the LM-BP equalizer keeps updating its weights and biases in each iteration until the desired error value or maximum number of iterations is reached.

In this paper LM-BP neural network algorithm is learned online. Its input and output are the PAM4 signal before and after transmission respectively. In this paper, the PAM4 signal itself is used as a sample and the number of samples is 65 536. The SSM part of this algorithm is carried out in Optisystem simulation software and a PAM4 signal IM-DD based system with SSM is built using Optisystem. The neural network equalization part is carried out offline with the help of Matlab. The fiber and dispersion compensated fiber (DCF) simulation parameters are shown in Tab.1.

Tab.1 Parameters of simulation

Parameter	Value
Fiber length	80 km
Fiber dispersion	16 ps·nm^{-1}·km^{-1}
DCF length	16 km
DCF length dispersion	−80 ps·nm^{-1}·km^{-1}
Fiber loss	0.2 dB/km

Since the lesser the number of neurons in a neural network algorithm, the worse the fit, while too many neurons can also produce overfitting or increase the complexity. Therefore, the number of neurons used in this algorithm is 5.

Subsequently, neural network equalization was implemented for two different nonlinear simulation modes, as depicted in Fig.6. The results indicate that the neural network exhibits a certain compensation effect on both nonlinear simulation distortions. However, as the nonlinearity increases (the eye chart distortion increases), the compensation effect appears to significantly decline.

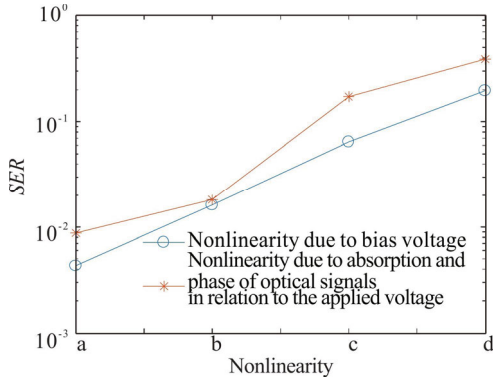

Fig.6 *SER* graph of LM-BP algorithm

As shown in Fig.7 and Fig.8, the SSM is used to equalize the two nonlinearities in Fig.1 and Fig.3. The SSM effectively equalizes the nonlinearities caused by the bias voltage, but it is less effective in equalizing larger nonlinearities resulting from changes in the absorption and phase of the optical signal in each arm of the modulator in relation to the applied voltage. Consequently, it does not result in a uniform eye diagram.

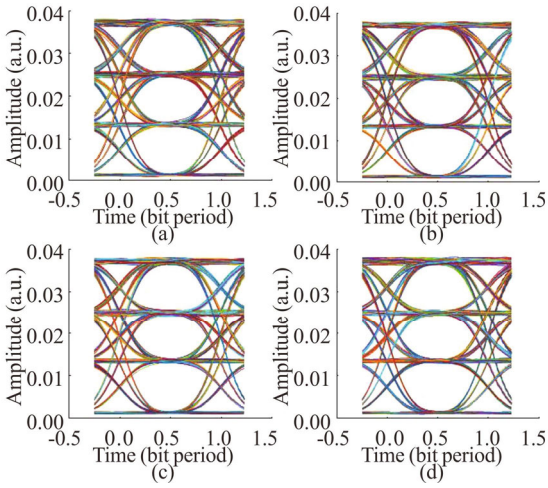

Fig.7 Four sets of nonlinear eye diagrams due to SSM equalization bias voltage: (a) V_{bias1}=3 V, V_{bias2}=−1.4 V; (b) V_{bias1}=3 V, V_{bias2}=−1.3 V; (c) V_{bias1}=3 V, V_{bias2}=−1.2 V; (d) V_{bias1}=3 V, V_{bias2}=−1.1 V

It can be observed that the equalization effect of the SSM is quite satisfactory, but the SSM equalization requires higher amplitude accuracy for the addition of sinusoidal subcarrier modulation. When it comes to nonlinearity caused by the absorption of the optical signals in each arm of the modulator and changes in phase relative to the applied voltage, this type of larger nonlinearity cannot be effectively equalized using the SSM alone, resulting in an incomplete eye diagram compensation. So the use of the

SSM-LM-BP scheme becomes a more suitable option. Initially, the larger nonlinearity is partially equalized using sinusoidal subcarrier modulation to mitigate nonlinearity, followed by precise equalization using the LM-BP algorithm.

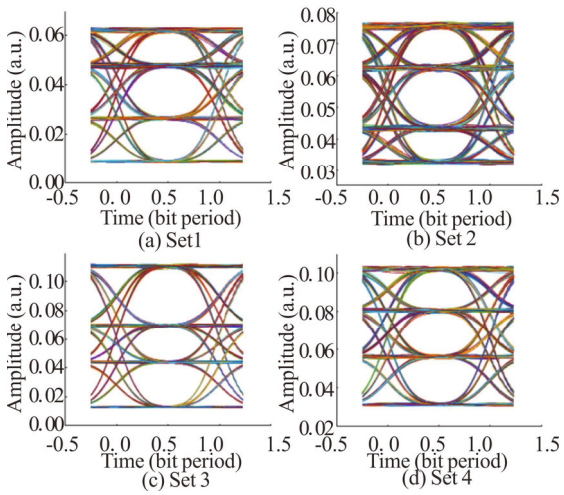

Fig.8 Four sets of nonlinear eye diagrams of the optical signal absorption and phase of each arm of the SSM equalized modulator as a function of the applied voltage

Fig.9 presents the symbol error rate (*SER*) curves for the joint method used to compensate for the two nonlinearities. The simulation results indicate that the joint scheme achieves excellent equalization effects for both the nonlinear distortion caused by the external bias voltage and the larger nonlinear distortion resulting from the absorption of optical signals in each arm of the modulator and the changes in phase relative to the applied voltage. Notably, the *SER* can reach the 10^{-5} order of magnitude, indicating a highly effective compensation.

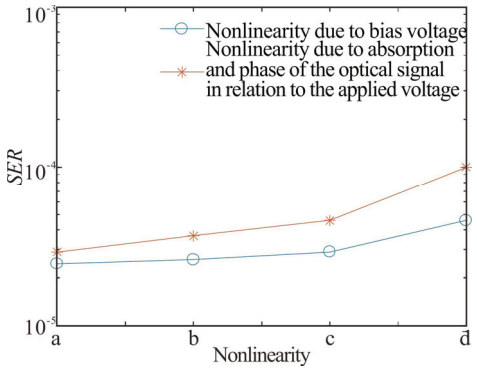

Fig.9 *SER* graph of the SSM-LM-BP

Next, we compare the performance of the four algorithms: SSM-LM-BP, LM-BP, SSM, and triangular subcarrier modulation (TSM), at the same transmission distance. Fig.10 and Fig.11 illustrate the relationship between *SER* and received optical power for the four algorithms when the transmission distance is 80 km, considering the two nonlinearities exemplified in Fig.1(a) and Fig.3(a), respectively.

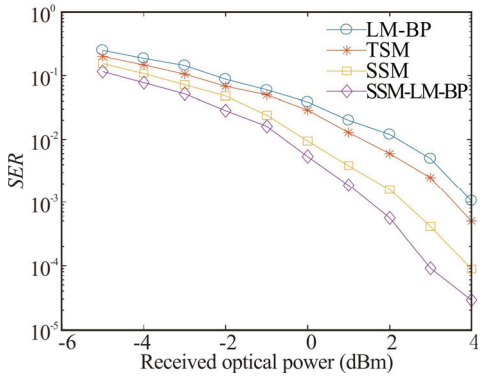

Fig.10 Comparison of nonlinearities caused by different methods of equalizing bias voltage for 50 Gbit/s PAM4 transmission over 80-km-long SSMF

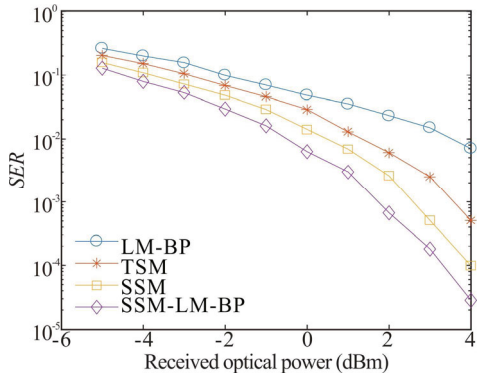

Fig.11 Comparison of nonlinearities induced by the absorption and phase of the optical signal per arm of different methods of equalizing the modulator with respect to the applied voltage for 50 Gbit/s PAM4 transmission over 80-km-long SSMF

As evident from Fig.10 and Fig.11, when the received optical power is low, the received signal is more susceptible to noise, leading to similar performance among the four algorithms. As the received optical power increases to 2 dBm, the primary factor impacting the signal transitions from noise to ISI. In this scenario, the joint algorithm significantly outperforms the other three algorithms for both nonlinearities. Moreover. TSM performs worse than SSM.

In this paper, the principle of electro-optic modulation of PAM4 signals in an IM-DD system is derived. To mitigate the impact of nonlinear impairments on the signals due to electro-optic modulation devices, a SSM-LM-BP based on IM-DD system is proposed. The joint SSM-LM-BP scheme is less complex to implement and exhibits superior *SER* performance. Through experimental analysis and comparison, the results show that with dispersion compensation, the joint scheme is still able to achieve an *SER* of 10^{-5} when transmitting 50 Gbit/s PAM4 signals over 80 km without relaying.

Ethics declarations

Conflicts of interest

The authors declare no conflict of interest.

References

[1] ZHOU J, WANG H D, WEI J L, et al. Adaptive moment estimation for polynomial nonlinear equalizer in PAM8-based optical interconnects[J]. Optics express, 2019, 27(22): 32210-32216.

[2] NEBOJSA S, FOTINI K, ZHANG Q, et al. Volterra and wiener equalizers for short-reach 100G PAM-4 applications[J]. Journal of lightwave technology, 2017, 35(21): 4583-4594.

[3] GIACOUMIDIS E, WEI J L, MHATLI S, et al. Nonlinear inter-subcarrier intermixing reduction in coherent optical OFDM using fast machine learning equalization[C]//2017 Optical Fiber Communications Conference and Exhibition: OFC 2017, March 19-23, 2017, Los Angeles, California, USA. New York: IEEE, 2017: W3J.2.

[4] FU J J, AHI Z, ZHANG Z F. 128 Gbit/s high speed optical interconnection networks in data centers by a 30 GHz Mach-Zehnder modulator[J]. Optoelectronics letters, 2023, 19(1): 36-40.

[5] NAVID H, ADITYA J, ROGER H, et al. A distributed low-noise amplifier for broadband linearization of a silicon photonic Mach-Zehnder modulator[J]. IEEE journal of solid-state circuits, 2021, 56(6): 1897-1909.

[6] ZHOU Z Y, ZHANG Q. A scheme for suppressing non-linear influence of Mach-Zehnder modulatorin RoF system[J]. Journal of optoelectronics·laser, 2021, 32(3): 223-230. (in Chinese)

[7] LUO Y L, RADY R, ENTESARI K, et al. A power-efficient 20-35-GHz MZM driver with programmable linearizer for analog photonic links in 28-nm CMOS[J]. IEEE transactions on microwave theory and techniques, 2023, 71(3): 1262-1273.

[8] LI L, LIU R, SUN Y D. A nonlinear equalization for a PAM4 IM-DD system using MZM[J]. Optoelectronics letters, 2022, 18(4): 238-242.

[9] LYUBOMIRSKY I, LING W. Advanced modulation for datacenter interconnect[C]//2016 Optical Fiber Communications Conference and Exhibition, March 20-24, 2016, Anaheim, California, USA. New York: IEEE, 2016: w4j3.

[10] NEBOJSA S, ZHANG Q, CRISTIAN P, et al. Performance and DSP complexity evaluation of a 112-Gbit/s PAM-4 transceiver employing a 25-GHz TOSA and ROSA[C]//2015 European Conference on Optical Communication (ECOC), September 27-October 1, 2015, Valencia, Spain. New York: IEEE, 2015: 7341947.

[11] YE C, ZHANG D G, HUANG X A, et al. Demonstration of 50Gbps IM-DD PAM4 PON over 10GHz class optics using neural network based nonlinear equalization[C]//2017 European Conference on Optical Communication (ECOC), September 17-21, 2017, Gothenburg, Sweden. New York: IEEE, 2017: 8346196.

[12] ZHANG J, JIANG L, LUO B, et al. 56-Gbit/s PAM-4 optical signal transmission over 100-km SMF enabled by TCNN regression model[J]. IEEE photonics journal, 2021, 13(4): 1-6.

[13] REZA A G, RHEE J K K. Nonlinear equalizer based on neural networks for PAM-4 signal transmission using DML[J]. IEEE photonics technology letters, 2018, 30(15): 1416-1419.

[14] WANG S B, YUAN W H, ZHOU J W. Analysis of run-off coefficient prediction based on LM-BP neural network[J]. Journal of physics: conference series, 2022, 2333: 012020.